nection with the boundary layer on a yawed moving plate. The leading term for $f(\eta)$, in the boundary layer, is easily

$$f = \varphi_0''(\zeta)/\varphi_0''(0) \tag{12}$$

This fact was first noticed by Rott [4] and Glauert [5] in their work on stagnation flow toward a moving plate.

Results and Discussion

Using an inverse method similar to reference [1], equations (2)–(6) are integrated numerically. The results are tabulated in Table 1. The approximate values compare fairly well with the exact values. Using the velocity, lift and drag can be found

$$L = \left(\frac{\rho W^4 L_2 L_1^3}{12\nu^2}\right)\left(\frac{-h'''(0)}{R^3}\right) \tag{13}$$

$$D_x = (\rho U W L_1 L_2)\left(\frac{-f'(1)}{R}\right) \tag{14}$$

$$D_y = (\rho V W L_1 L_2)\left(\frac{-g'(1)}{R}\right) \tag{15}$$

We can deduce the following theoretical results for the two-dimensional slider. First, for the same slider surface area (L_1L_2), lift increases more if L_1 is increased (circular slider is still optimum). Drag however is not affected by the aspect ratio. Second, if the slider dimensions are fixed, drag is lower if the slider is translating crosswise along the x-direction, since in general $-f'(1) < -g'(1)$. The normalized lift and drag are plotted in Fig. 1. As in the axisymmetric case, both lift and drag are quite sensitive to the Reynolds number. The minimum lift to drag ratio occurs near $R = 4$ where slider operation should be avoided.

References

1 Wang, C.-Y., "Fluid Dynamics of the Circular Porous Slider," JOURNAL OF APPLIED MECHANICS, Vol. 41, TRANS. ASME, Vol. 96, Series E, 1974, pp. 343–347.

2 Hiemenz, K., "Die Grenzschicht an einem in den gleichförmigen Flüssigkeitsstrom eingetauchten geraden Kreiszylinder," *Dinglers Journal*, Vol. 326, 1911, pp. 321–410.

3 Prandtl, L., "Ueber Reibungsschichten bei dreidimensionalen Strömung," *Betz Festschr.*, Gottingen, 1945, Rep. Aero. Res. Coun., London, No. 9828, 1946.

4 Rott, N., "Unsteady Viscous Flow in the Vicinity of a Stagnation Point," *Quarterly of Applied Mathematics*, Vol. 13, 1956, pp. 444–451.

5 Glauert, M. B., "The Laminar Boundary Layer on Oscillating Plates and Cylinders," *Journal of Fluid Mechanics*, Vol. 1, 1956, pp. 97–110.

Instability of Clamped-Hinged Circular Arches Subjected to a Point Load

D. A. DaDeppo[1] and R. Schmidt[2]

This Note presents the results of an investigation of stability of nonshallow circular arches whose one end is clamped and the other hinged. The analysis is based on Euler's nonlinear theory of the inextensible elastica. This theory is exact in the sense that no restrictions are placed on the magnitudes of deflections. It has been found that, in the case of a downward concentrated load acting on the crown, a high-rise elastic arch becomes unstable after large prebuckling deflections. The load-deflection curve displays a maximum at the point of instability.

The problem of possible instabilities of arches after *large asymmetrical* prebuckling deflections was considered only once before [1],[3] by Deutsch in 1940. Deutsch experimentally investigated two-hinged and hingeless parabolic arches subjected to asymmetrically stepped distributed loads. According to [2], the exact nature of the buckling phenomenon was not clear; however, Deutsch reported substantially reduced buckling strengths for unsymmetrically loaded arches as compared to the same arches under a uniformly distributed (symmetric) load.

For a nearly complete bibliography of buckling of arches see [3, 4].

The results presented herein were obtained by means of the nonlinear equations and the method of their solution described in [5].

Calculated Results

Let us introduce the following notation: a = radius of the undeformed (circular) centroidal curve, E = modulus of elasticity, I = moment of inertia of cross-sectional area, P = downward point load at the crown, u = horizontal displacement of the crown point C, v = downward displacement of C, 2α = subtending angle of the arch, and β = angle of rotation of the tangent at the crown. Next, let us calculate the values of various selected quantities in terms of a load parameter and plot the results.

Graphs of Pa^2/EI versus v/a, i.e., dimensionless load versus dimensionless downward displacement of the load, reach a maximum before any bifurcations take place in all cases considered, i.e., for all values of the subtending angle 2α between 60° and 260° (e.g., see Figs. 1–4). Hence, by a critical or buckling load we mean herein the so-called upper-limit load. Its values are presented in

Table 1 Critical values of load and displacement parameters for different magnitudes of subtending angle 2α

α (degrees)	$\frac{Pa^2}{EI}$	$\frac{u}{a}$ →	$\frac{v}{a}$ ↓	β ↻
30	24.75	0.0113	0.0693	0.1362
40	18.87	0.0266	0.1260	0.1760
50	15.42	0.0515	0.2038	0.2118
60	13.21	0.0881	0.3061	0.2429
70	11.74	0.1384	0.4386	0.2691
80	10.78	0.2038	0.6074	0.2895
90	10.27	0.2869	0.8178	0.3017
95	10.23	0.3375	0.9410	0.3024
100	10.42	0.3995	1.0802	0.2942
102.5	10.71	0.4398	1.1599	0.2808
105	11.47	0.5097	1.2580	0.2266
105.3125	11.05	0.5649	1.2228	0.1269
105.625	10.60	0.5761	1.2013	0.1056
106.25	9.94	0.5907	1.1739	0.0890
107.5	8.97	0.6116	1.1372	0.0498
110	7.58	0.6438	1.0866	0.0078
115	5.72	0.6940	1.0136	-0.0529
120	4.47	0.7340	0.9554	-0.1031
130	2.86	0.7994	0.8714	-0.1949

[1] Professor, Department of Civil Engineering and Engineering Mechanics, The University of Arizona, Tucson, Ariz. Mem. ASME.

[2] Professor of Engineering Mechanics, Department of Civil Engineering, University of Detroit, Detroit, Mich. Mem. ASME.

[3] Numbers in brackets designate References at end of Note.

Manuscript received by ASME Applied Mechanics Division, March, 1975.

 Copyright © 1975 by ASME

Downloaded From: http://appliedmechanics.asmedigitalcollection.asme.org/ on 01/29/2016 Terms of Use: http://www.asme.org/about-asme/terms-of-use

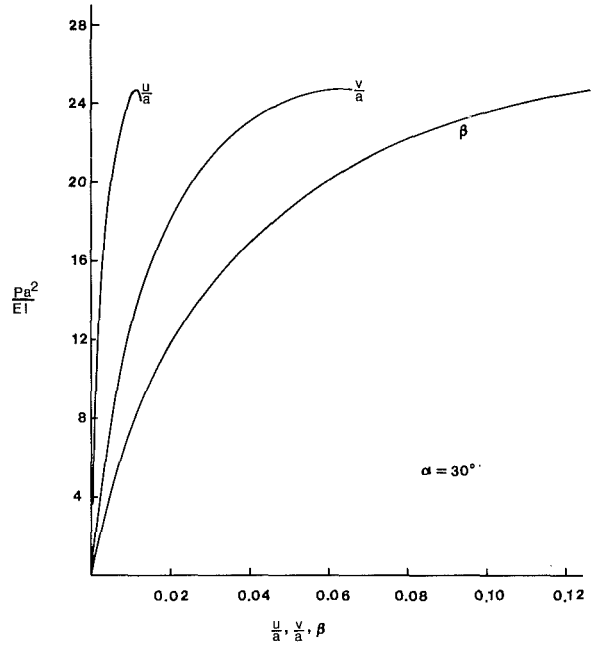

Fig. 1

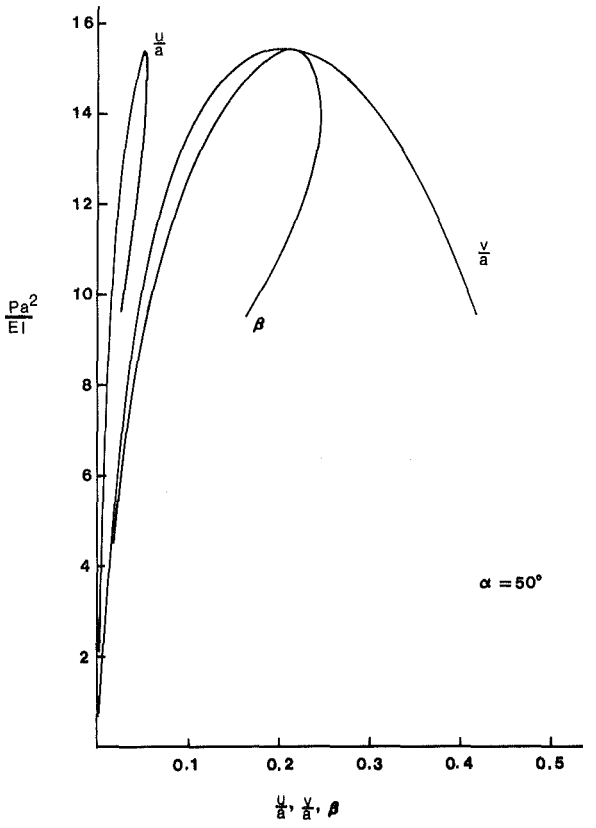

Fig. 2

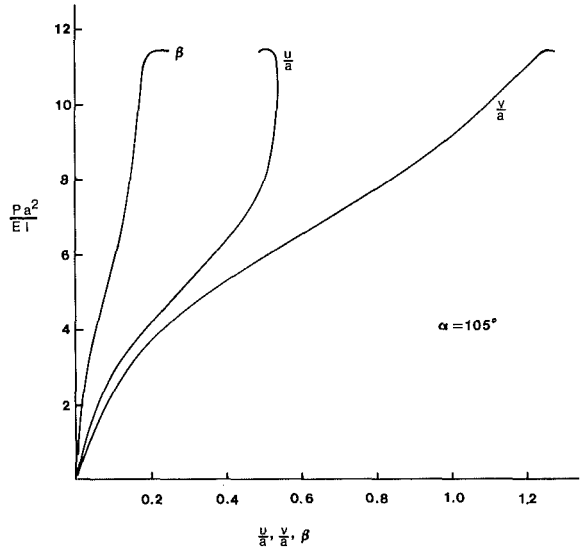

Fig. 3

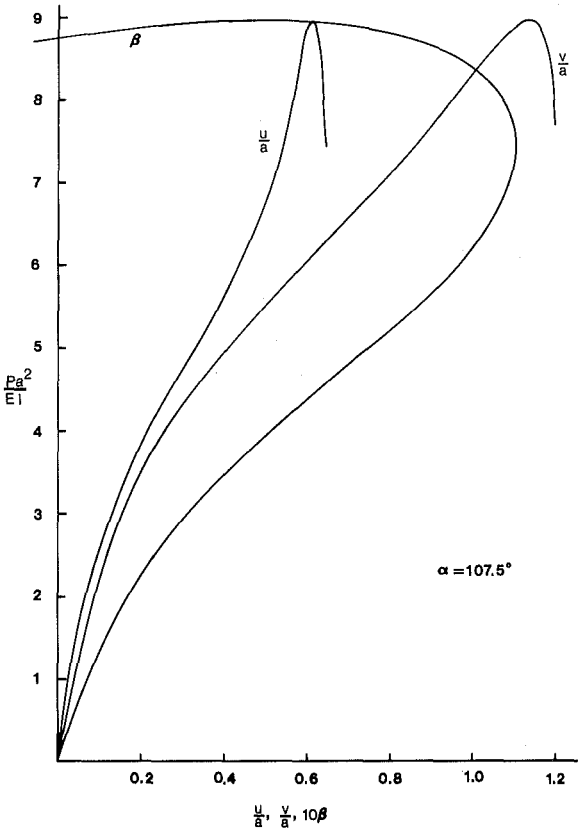

Fig. 4

Table 1 and Fig. 5. We observe that, for $\alpha \simeq 105$ deg, the P_{cr} versus α plot displays a cusp at which, seemingly, two different smooth curves meet along a vertical tangent. Examining the load-displacement curves for $\alpha = 105$ deg in Fig. 3, we note that, after very large prebuckling deflections, when the crown and, therefore, the load are approaching the level of supports, the arch configuration is such as not to permit a farther increase in the horizontal displacement of the arch crown.

Acknowledgment

This investigation was supported by the National Science Foundation grant GK-19726.

References

1 Deutsch, E., "Das Knicken von Bogenträgern bei unsymmetrischer Belastung," *Der Bauingenieur*, Vol. 21, No. 45/46, Dec. 1940, pp. 353–360.

2 Austin, W. J., "In-Plane Bending and Buckling of Arches," *Journal of the Structural Division, Proceedings ASCE*, Vol. 97, No. ST5, May 1971, pp. 1575–1592.

3 DaDeppo, D. A., and Schmidt, R., "Stability of an Arch Under Combined Loads; Bibliography on Stability of Arches," *Industrial Mathematics*,

Downloaded From: http://appliedmechanics.asmedigitalcollection.asme.org/ on 01/29/2016 Terms of Use: http://www.asme.org/about-asme/terms-of-use

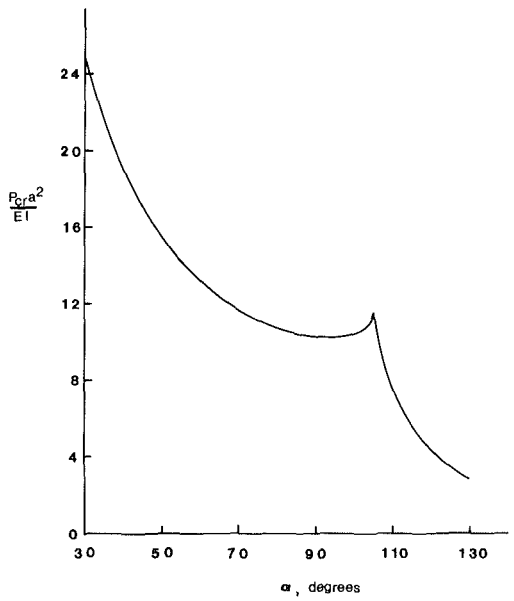

Fig. 5

The Journal of the Industrial Mathematics Society, Vol. 20, Part 2, 1970, pp. 71–89.

4 Schmidt, R., and DaDeppo, D. A., "A Survey of Literature on Large Deflections of Nonshallow Arches. Bibliography of Finite Deflections of Straight and Curved Beams, Rings, and Shallow Arches," *Industrial Mathematics, The Journal of the Industrial Mathematics Society,* Vol. 21, Part 2, 1971, pp. 91–114.

5 DaDeppo, D. A., and Schmidt, R., "Large Deflections and Stability of Hingeless Circular Arches Under Interacting Loads," JOURNAL OF APPLIED MECHANICS, Vol. 41, No. 4, TRANS. ASME, Vol. 96, Series E, Dec. 1974, pp. 989–994.

Axially Symmetric Stress Distributions in Elastic Solids Containing Penny-Shaped Cracks Under Torsion

M. L. Pasha[1]

We present the axially symmetric stress distributions in elastic solids containing a pair of axially symmetric penny shaped cracks when the infinite elastic medium is kept under torsion. We derive the integral representation formula for the torsion function and the expressions for the stress-intensity factors.

Introduction

Recently, in a joint paper, the author [1][2] discussed the problem of axially symmetric stress distributions in elastic solids containing ring-shaped cracks under torsion. All other relevent references can be obtained from reference [1]. The problem of stress distributions in elastic solids under torsion due to two or more axially symmetric penny shaped cracks is of equal importance and interest and forms the topic of this Note.

Statement and Mathematical Formulation of the Problem

Let a pair of axially symmetric penny-shaped cracks be situated inside an infinite, homogeneous, and isotropic elastic solid which is maintained under torsion by a torque applied about the axis of symmetry of the cracks. The definition of the crack is that it separates the material and there is no stress across it. Cylindrical polar coordinates (ρ,ϕ,z) are chosen with z-axis as the axis of symmetry of the cracks such that the cracks are given by

$$z = 0, 0 \leq \rho < a_1, \text{ and } z = f, 0 \leq \rho < a_2 \tag{1}$$

The only nonvanishing stress components are [1]

$$\sigma_{z\phi} = \mu\tau\rho + \frac{\mu}{\rho^2}\frac{\partial}{\partial\rho}(\rho^2\Psi); \; \sigma_{\rho\phi} = -\mu\frac{\partial\Psi}{\partial z} \tag{2}$$

where $\Psi(\rho,z)$ is the torsion function and τ is the angle of twist per unit length. From [1] it follows that $\Psi(\rho,z)$ satisfies the boundary-value problem

$$\nabla^2(\Psi\cos 2\phi) = 0, \; (\rho, \phi, z) \text{ not on the cracks}, \tag{3}$$

$$\Psi(\rho, 0)\cos 2\phi = -\tau\rho^2\cos 2\phi/4, \quad 0 \leq \rho < a_1;$$

$$\Psi(\rho, f)\cos 2\phi = -\tau\rho^2\cos 2\phi/4, \quad 0 \leq \rho < a_2. \tag{4}$$

Boundary conditions (4) follow from the assumption that there is no stress across the faces of the cracks. The integral representation formula for $\Psi(\rho,z)$ is [2]

$$\Psi(\rho, z)\cos 2\phi = \int_0^{a_1}\int_0^{2\pi}\frac{l\sigma_1(l)\cos 2\phi'\, d\phi'\, dl}{[z^2 + l^2 + \rho^2 - 2\rho l\cos(\phi - \phi')]^{1/2}} + \int_0^{a_2}\int_0^{2\pi}\frac{l\sigma_2(l)\cos 2\phi'\, d\phi'\, dl}{[(z - f)^2 + l^2 + \rho^2 - 2\rho l\cos(\phi - \phi')]^{1/2}}, \tag{5}$$

where $\sigma_1(t)$ and $\sigma_2(t)$ are the charge densities defined as

$$\sigma_1(l) = \frac{1}{4\pi}\left[\frac{\partial(l, z_1)}{\partial z_1}\Big|_{z_1=0-} - \frac{\partial(l, z_1)}{\partial z_1}\Big|_{z_1=0+}\right], \quad 0 \leq l < a_1, \tag{6}$$

$$\sigma_2(l) = \frac{1}{4\pi}\left[\frac{\partial(l, z_1)}{\partial z_1}\Big|_{z_1=f-} - \frac{\partial(l, z_1)}{\partial z_1}\Big|_{z_1=f+}\right], \quad 0 \leq l < a_2, \tag{7}$$

and (t,ϕ',z_1) denotes the source point. Applying the boundary conditions and after a slight simplification, we derive a pair of integral equations which will be used to determine the charge densities $\sigma_1(t)$ and $\sigma_2(t)$. The pair of integral equations is

$$-\frac{1}{4}\tau\rho^2 = \int_0^{a_i} l\sigma_i(l)\, dl\int_0^{2\pi}(\rho^2 + l^2 - 2\rho l\cos\psi)^{-1/2}\times\cos 2\psi\, d\psi + \int_0^{a_j} l\sigma_j(l)\, dl\int_0^{2\pi}(\rho^2 + l^2 + f^2 - 2\rho l\cos\psi)^{-1/2}\times\cos 2\psi d\psi, \; 0 \leq \rho < a_i; \; i = 1, 2; \; j = 3 - i, \tag{8}$$

where repeated indices do not imply summation.

Once the charge densities are determined, (5) will give the integral representation formula for $\Psi(\rho,z)$.

Solution

Let us define four unknown functions $S_i(w)$, and $F_i(w)$; $i = 1,2$, as follows:

$$S_i(w) = w^2\int_w^{a_i} l^{-1}(l^2 - w^2)^{-1/2}\sigma_i(l)\, dl, \; 0 \leq w < a_i, \tag{9}$$

$$-\tau w^2/4 = 4w^{-2}\int_0^w l^2(w^2 - l^2)^{-1/2}F_i(l)\, dl, \quad 0 \leq w < a_i. \tag{10}$$

[1] Research Associate, Department of Petroleum and Natural Gas Engineering, Pennsylvania State University, University Park, Pa.

[2] Numbers in brackets designate References at end of Note.

Manuscript received by ASME Applied Mechanics Division, March, 1975; final revision, May, 1975.

Downloaded From: http://appliedmechanics.asmedigitalcollection.asme.org/ on 01/29/2016 Terms of Use: http://www.asme.org/about-asme/terms-of-use